

Trajectory Formation Based on the Minimum Commanded Torque Change Model Using the Euler–Poisson Equation

Yuichi Kaneko,¹ Eri Nakano,² Rieko Osu,³ Yasuhiro Wada,¹ and Mitsuo Kawato^{3,4}

¹Nagaoka University of Technology, Nagaoko, 940-2188 Japan

²Advanced Telecommunications Research Institute International, Kyoto, 619-0288 Japan

³ERATO Kawato Dynamic Brain Project, Kyoto, 619-0288 Japan

⁴ATR Human Information Processing Research Laboratories, Kyoto, 619-0288 Japan

SUMMARY

A minimum commanded torque change criterion based on the optimization principle is proposed as a model that accounts for human voluntary motion. It is shown that the trajectory of human arm motion can be well reproduced by the model. In the point-to-point movement, the calculation of the torque based on the minimum commanded torque change criterion requires a highly nonlinear calculation, and it is difficult to determine the optimal trajectory. As solution methods, a Newton-like method and a steepest descent method have been proposed. However, an optimal solution cannot be obtained by these methods, for several reasons. This paper proposes a method in which the trajectory of the joint angle is analytically represented by a system of orthogonal polynomials, and the coefficients of the orthogonal polynomials are estimated by a linear iterative calculation so that the parameters satisfy the Euler–Poisson equation, as a necessary condition for the optimal solution. As a result of numerical experiments, it is shown that a solution satisfying the Euler–Poisson equation with high numerical accuracy is obtained in a short time, regard-

less of the parameters such as those of the boundary conditions. © 2005 Wiley Periodicals, Inc. *Syst Comp Jpn*, 36(2): 92–103, 2005; Published online in Wiley InterScience (www.interscience.wiley.com). DOI 10.1002/scj.20014

Key words: minimum commanded torque change criterion; Euler–Poisson equation; system of orthogonal polynomials; trajectory generation; optimization.

1. Introduction

The following two properties have been pointed out as features of point-to-point human movement in multijoint arm movement [1]:

- (1) The trajectory is slightly curved although almost straight.
- (2) The velocity profile with respect to time exhibits a single-peaked bell shape.

Several models have been proposed in order to account for these features [2–6]. They include the minimum hand jerk criterion [2], the minimum angle jerk criterion [3], the minimum torque change criterion [4], and the minimum

Contract grant sponsor: Supported in part by a grant from the Science and Technology Agency under the project “Study of Communication of Primates, Including Humans.”

commanded torque change criterion [5], which are trajectory based on the optimization principle.

Among these methods, an analytical solution can be derived relatively easily for the minimum hand jerk criterion and the minimum angle jerk criterion. The others are models in which the torque change is made smooth based on the arm dynamics. A constrained nonlinear optimization problem must be solved, minimizing the evaluation function under the constraints (nonlinear dynamics) and the boundary conditions (start and goal). Generally, it is very difficult to derive a solution for these problems. The minimum commanded torque change criterion is considered as a criterion that effectively reproduces human motion. It has been reported by Nakano and colleagues [5] and Sakuraba and colleagues [7] that the minimum commanded torque change criterion predicts the human trajectory better than any other of these criteria.

However, for this criterion, it is difficult to establish a method that can derive the optimal trajectory stably for various starts, goals, and dynamical parameters. It is an important issue to establish such a method. Existing algorithms that try to derive the trajectory include the Newton-like method [3, 9] and the steepest descent method [5]. In the Newton-like method, it is guaranteed mathematically that the convergence result is the optimal solution. However, the algorithm may become unstable and often diverges, depending on the dynamical parameter that represents the viscosity. Furthermore, assuming that the initial value of the Newton-like method may have an effect, the solution is sought by modifying the method of estimation of the initial value [10]. It has been found that there are many trajectories for which convergence is not achieved.

In the method of steepest descent, on the other hand, the solution can be derived stably, but the optimality of the solution is not guaranteed. A hybrid method that combines these methods has also been proposed [10]. However, this method cannot eliminate the above difficulty concerning the Newton-like method.

It is indispensable to find the optimal solution in the mathematical model that tries to account for human arm movement based on the optimality principle. It is also highly desirable to have an algorithm that can calculate the optimal trajectory reliably and accurately with the minimum commanded torque change criterion. Nakano and colleagues [5] and Sakuraba and colleagues [7] found that it is difficult to determine the optimal trajectory with the minimum commanded torque change, and had to compare the quasioptimal trajectory with the minimum commanded torque change derived by the method of steepest descent and the optimal trajectory obtained by another criterion. In order to clarify these points, it is important to establish an algorithm that can derive the minimum commanded torque change trajectory.

This paper takes an approach which differs from the past proposals. An algorithm is proposed that calculates the trajectory that satisfies with high accuracy the Euler–Poisson equation, representing the necessary condition for the optimal solution, based on the minimum commanded torque change criterion. The trajectory of the joint angle is represented by a system of polynomials in time, so that the boundary conditions are always strictly satisfied. The Euler–Poisson equation is derived from the boundary conditions and the functional optimal problem. By iterating linear operations of the coefficients of the above polynomials, the Euler–Poisson equations are satisfied with high accuracy. In the conventional methods (i.e., the Newton-like method and steepest descent method), it is not always true that the derived trajectory strictly satisfies the boundary conditions. It has been difficult to solve this point. But in the proposed method, a trajectory is determined that strictly satisfies the boundary conditions and satisfies the Euler–Poisson equation with high accuracy.

For the case of two-joint arm movement in each plane (i.e., the horizontal plane and the sagittal plane), a numerical experiment has been performed to generate the minimum commanded torque change trajectory. The result has been reported, indicating that the proposed method can quickly derive a solution that satisfies the Euler–Poisson equation with high accuracy. It has also been shown that a solution is obtained which is robust to changes of the start and the goal of the trajectory, and to changes of the dynamical parameters of the arm.

2. Computation Algorithm for Minimum Commanded Torque Change Trajectory Using the Euler–Poisson Equation

2.1. The minimum commanded torque change criterion

In the minimum commanded torque change criterion, the trajectory is planned so that the time change of the commanded torque τ_i of each joint i is minimized. The evaluation function is given

$$C_{CTC} = \frac{1}{2} \int_0^{t_f} \sum_{i=1}^N \left(\frac{d\tau_i}{dt} \right)^2 dt \quad (1)$$

Here, t_f is the duration of motion and N is the number of joints. The trajectory of the movement between two points is generated by this criterion, considering the dynamical parameters such as the mass and the moment of inertia of the arm as shown in Eq. (2). The features of the motion trajectory generated by this criterion depend on the positions of movement (start and goal).

In this paper, the trajectory of a two-link two-joint arm is generated on:

- (a) the horizontal plane at the same height as the shoulder or the elbow joint, and
- (b) the sagittal plane perpendicular to the segment connecting both shoulders.

Equation (2) is used in the calculation of the commanded torque of each joint. In the following, the n -th time derivative of θ_i ($i = 1, 2$) is written as $\theta_i^{(n)}$. We see that the expression for the commanded torque is highly nonlinear, including triangular functions and the squares of the joint angles:

$$\begin{aligned}
\tau_1 &= \{I_1 + I_2 + 2M_2L_1S_2 \cos \theta_2 + M_2(L_1)^2\} \theta_1^{(2)} \\
&\quad + (I_2 + M_2L_1S_2 \cos \theta_2) \theta_2^{(2)} \\
&\quad - M_2L_1S_2(2\theta_1^{(1)} + \theta_2^{(1)}) \theta_2^{(1)} \sin \theta_2 \\
&\quad + B_{11}\theta_1^{(1)} + B_{12}\theta_2^{(1)} \\
&\quad + g \{(M_1S_1 + M_2L_1) \sin \theta_1 \\
&\quad + M_2S_2 \sin(\theta_1 + \theta_2)\} \\
\tau_2 &= (I_2 + M_2L_1S_2 \cos \theta_2) \theta_1^{(2)} + I_2\theta_2^{(2)} \\
&\quad + M_2L_1S_2(\theta_1^{(1)})^2 \sin \theta_2 + B_{22}\theta_2^{(1)} + B_{21}\theta_1^{(1)} \\
&\quad + gM_2S_2 \sin(\theta_1 + \theta_2)
\end{aligned} \tag{2}$$

Here τ_1 and θ_1 are respectively the commanded torque and the joint angle, of the shoulder joint, and τ_2 and θ_2 are those of the elbow joint. I_i , M_i , L_i , and S_i are the moment of inertia around the joint, the mass, the length, and the distance from the joint to the center of gravity, of the link i ($i = 1, 2$). B_{ij} represents the viscosity, which expresses the effect of the joint angle velocity of link j ($j = 1, 2$) on link i . Link 1 is the upper arm and link 2 is the forearm. In the motion on the sagittal plane [Fig. 1(b)], there is an effect of gravity on the rotation of the joint. g is set as the gravity acceleration (9.8 m/s^2) and the commanded torque is calculated. In the case

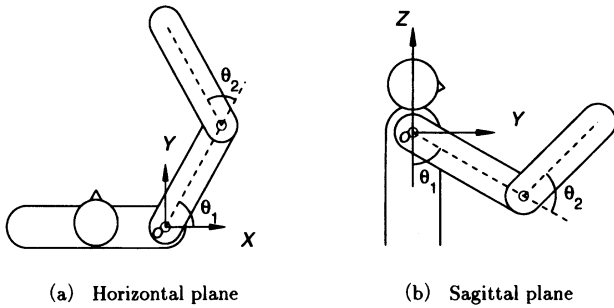


Fig. 1. Movement plane.

of the horizontal plane [Fig. 1(a)], the gravity force is perpendicular to the direction of rotation of the joint, and the effect of the gravity force can be ignored in the calculation of the commanded torque in the above direction. Consequently, we set $g = 0$ in the calculation.

The commanded torque calculated by this criterion is not the mechanical output torque, but is the torque that can be considered as an approximation to the motor command [5].

2.2. The Euler–Poisson equation

This section describes the algorithm for computing the trajectory based on the minimum commanded torque change criterion using the Euler–Poisson equation. The essential aspect of the proposed algorithm is to use the polynomials in time of the joint angle trajectory to approximate the function that satisfies the Euler–Poisson equation derived from the minimum commanded torque change criterion. The evaluation function for the minimum commanded torque change criterion [Eq. (1)] is

$$\begin{aligned}
C_{CTC} &= \frac{1}{2} \int_0^{t_f} F(t, \theta_1, \theta_2, \theta_1^{(1)}, \theta_2^{(1)}, \theta_1^{(2)}, \theta_2^{(2)}, \theta_1^{(3)}, \theta_2^{(3)}) dt \\
&\rightarrow Min
\end{aligned} \tag{3}$$

$$\text{where } F = \sum_{i=1}^2 \left(\frac{-d\tau_i}{dt} \right)^2.$$

Applying the method of variation under the boundary conditions at the start and the goal (position, velocity, and acceleration), the following Euler–Poisson equations are derived as the necessary condition for the extremum of the evaluation function:

$$\begin{aligned}
\frac{\partial}{\partial \theta_1} F - \frac{d}{dt} \frac{\partial}{\partial \theta_1^{(1)}} F + \frac{d^2}{dt^2} \frac{\partial}{\partial \theta_1^{(2)}} F - \frac{d^3}{dt^3} \frac{\partial}{\partial \theta_1^{(3)}} F \\
= 0 \\
\frac{\partial}{\partial \theta_2} F - \frac{d}{dt} \frac{\partial}{\partial \theta_2^{(1)}} F + \frac{d^2}{dt^2} \frac{\partial}{\partial \theta_2^{(2)}} F - \frac{d^3}{dt^3} \frac{\partial}{\partial \theta_2^{(3)}} F \\
= 0
\end{aligned} \tag{4}$$

θ_1 and θ_2 satisfying the above two Euler–Poisson equations at any time in the movement duration give the minimum commanded torque change trajectory. Then the left-hand sides of Eq. (4) are defined as E_1 and E_2 , respectively:

$$\begin{aligned}
E_1 &= \frac{\partial}{\partial \theta_1} F - \frac{d}{dt} \frac{\partial}{\partial \theta_1^{(1)}} F + \frac{d^2}{dt^2} \frac{\partial}{\partial \theta_1^{(2)}} F \\
&\quad - \frac{d^3}{dt^3} \frac{\partial}{\partial \theta_1^{(3)}} F
\end{aligned}$$

$$E_2 = \frac{\partial}{\partial \theta_2} F - \frac{d}{dt} \frac{\partial}{\partial \theta_2^{(1)}} F + \frac{d^2}{dt^2} \frac{\partial}{\partial \theta_2^{(2)}} F - \frac{d^3}{dt^3} \frac{\partial}{\partial \theta_2^{(3)}} F \quad (5)$$

2.3. Time polynomial of the minimum commanded torque change trajectory

The commanded torque is approximated by using terms concerned only with moments of inertia I_1 and I_2 . Then Eq. (2) takes the form

$$\begin{aligned} \tau_1 &= \{I_1 + I_2\} \theta_1^{(2)} + I_2 \theta_2^{(2)} \\ \tau_2 &= I_2 \theta_1^{(2)} + I_2 \theta_2^{(2)} \end{aligned} \quad (6)$$

The minimum commanded torque change criterion based on Eq. (6) is equivalent to the minimum angle-jerk criterion [Eq. (9), described later].

At the above level of approximation, suppose that the minimum angle jerk trajectory is a trajectory approximating the minimum commanded torque change criterion. The minimum commanded torque change trajectory $\theta_i(t)$ ($i = 1, 2$) is represented as follows:

$$\theta_i(t) = \theta_i^{AJ}(t) + \Delta\theta_i(t) \quad (7)$$

where $\theta_i^{AJ}(t)$ is the minimum angle jerk trajectory and $\Delta\theta_i(t)$ is the difference between the minimum commanded torque change trajectory and the minimum angle jerk trajectory.

It is required that the trajectory expressed by Eq. (7) should satisfy the following boundary conditions at the start and end of movement:

$$\begin{aligned} \theta_i(0) &= \theta_i^s, \quad \theta_i^{(1)}(0) = \theta_i^{(2)}(0) = 0 \\ \theta_i(t_f) &= \theta_i^f, \quad \theta_i^{(1)}(t_f) = \theta_i^{(2)}(t_f) = 0 \quad (i = 1, 2) \end{aligned} \quad (8)$$

where θ_1^s and θ_2^s are the joint angles of the shoulder and the elbow, respectively, expressing the position of the start point. θ_1^f and θ_2^f are those indicating the position of the final point.

Next we present in detail the method of formulating the minimum angle jerk trajectory of the first term on the right-hand side of Eq. (7) and the difference trajectory of the second term.

2.3.1. The minimum angle jerk trajectory

$$\theta_i^{AJ}(t)$$

The minimum angle jerk trajectory is the trajectory which is planned on the basis of the minimum angle jerk criterion. In the minimum angle jerk criterion, the move-

ment is planned so that the smoothness of the trajectory in the joint angle space is enhanced for the entire motion duration. In other words, the jerk of the joint angle (the time derivative of the joint angle acceleration) is considered, and the integral of its square over the motion duration shown in Eq. (9) is minimized:

$$C_{AJ} = \frac{1}{2} \int_0^{t_f} \sum_{i=1}^2 \left(\frac{d^3 \theta_i}{dt^3} \right)^2 dt \quad (9)$$

where θ_i is the joint angle of joint i .

Based on this criterion, an analytic solution can be derived easily. Assuming that θ_1 and θ_2 are independent, the problem is to minimize the square integral of the jerk of each coordinate (i.e., the third-order time derivative). Then, the solution is a fifth-order spline function [11].

By normalizing the previously defined boundary conditions and the motion duration, the minimum angle jerk trajectory is determined as follows [2]:

$$\theta_i^{AJ}(t) = \theta_i^s + (\theta_i^s - \theta_i^f)(-10t^3 + 15t^4 - 6t^5) \quad (0 \leq t \leq 1) \quad (10)$$

The trajectory between two points is thus generated as a straight line in the joint angle space. By applying a coordinate transformation to transfer the above trajectory to the external space, the trajectory becomes a trajectory which is slowly curved.

2.3.2. Difference trajectory $\Delta\theta_i(t)$

We see from Eq. (7) that $\theta_i^{AJ}(t)$ in Eq. (10) already satisfies the boundary conditions for the position, velocity, and acceleration at the start and the goal [Eq. (8)]. Consequently, if the difference trajectory $\Delta\theta_i(t)$ is a function that satisfies the boundary conditions that all of the positions, velocities, and accelerations at the start and the goal are zero, $\Delta\theta_i(t)$ in Eq. (7) gives a trajectory that always strictly satisfies the boundary conditions. Consequently, in this method, the difference trajectory is formulated so that the positions, velocities, and accelerations at the start and the goal are zero.

Kaneko and colleagues [12] considered the following polynomial approximation as $\Delta\theta_i(t)$ satisfying the above condition:

$$t^3(1-t)^3 \sum_{k=0}^K a'_{ik} t^k \quad (11)$$

An algorithm is proposed in the next section in which the parameters a'_{ik} are estimated.

In the approximation by the method of least squares, however, the polynomial approximation by a power series

as in Eq. (11) leads to an ill-conditioned canonical equation [13], and the error of the coefficients is increased in the numerical calculation. To perform the approximation without increasing the error, it is effective to use a system of orthogonal polynomials [14]. In this paper, a method is proposed in which the Jacobi polynomials, a system of orthogonal polynomials, are used in formulating $\Delta\theta_i(t)$. The Jacobi polynomial is defined as follows [14].

Generally, consider a family of polynomials R_k ($k = 0, 1, 2, \dots$) defined on the interval $[a, b]$. If R_k and R_l satisfy

$$(R_k, R_l)_w = \int_a^b R_k(x)R_l(x)w(x)dx = 0 \quad (\text{where } k \neq l) \quad (12)$$

they are called a system of orthogonal polynomials with weight w on interval $[a, b]$.

In this case, the orthogonal polynomial is derived by a third-order recurrence formula [14]. In particular, consider the following weight $w(x)$ defined on the interval $(-1, 1)$:

$$w(x) = (1+x)^\alpha(1-x)^\beta \quad (\alpha, \beta > -1) \quad (13)$$

The series of functions $P_k^{(\alpha, \beta)}(x)$ ($k = 0, 1, \dots$) which are orthogonal with respect to Eq. (13) are the Jacobi polynomials.

Consider

$$(P_k^{(\alpha, \beta)}, P_l^{(\alpha, \beta)})_w = \int_{-1}^1 P_k^{(\alpha, \beta)}(x) (w(x))^{\frac{1}{2}} P_l^{(\alpha, \beta)}(x) (w(x))^{\frac{1}{2}} dx \quad (14)$$

Let

$$\begin{aligned} w(x) &= (1+x)^6(1-x)^6 \\ &= \{(1+x)^6(1-x)^6\}^{\frac{1}{2}} \{(1+x)^6(1-x)^6\}^{\frac{1}{2}} \\ &= (1+x)^3(1-x)^3(1+x)^3(1-x)^3 \end{aligned} \quad (15)$$

Then, the Jacobi polynomials $P_k^{(6,6)}(x)$ and $P_l^{(6,6)}(x)$ are orthogonal as follows:

$$\begin{aligned} (P_k^{(6,6)}, P_l^{(6,6)})_w &= \int_{-1}^1 \left\{ (1+x)^3(1-x)^3 P_k^{(6,6)}(x) \right\} \\ &\quad \cdot \left\{ (1+x)^3(1-x)^3 P_l^{(6,6)}(x) \right\} dx = 0 \\ &\quad (\text{where } k \neq l) \end{aligned} \quad (16)$$

In addition, $Q_k(x) = (1+x)^3(1-x)^3 P_k^{(6,6)}(x)$ satisfies

$$\begin{aligned} Q_k(-1) &= Q_k(1) = 0 \\ \left. \frac{dQ_k(x)}{dx} \right|_{x=-1} &= \left. \frac{dQ_k(x)}{dx} \right|_{x=1} = 0 \\ \left. \frac{d^2Q_k(x)}{dx^2} \right|_{x=-1} &= \left. \frac{d^2Q_k(x)}{dx^2} \right|_{x=1} = 0 \end{aligned} \quad (17)$$

at both ends of the interval $[-1, 1]$.

Applying the coordinate transformation $t = (x+1)/2$, $\tilde{Q}_k(t) = 64t^3(1-t)^3 \tilde{P}_k^{(6,6)}(t)$ is obtained. Let

$$\Delta\theta_i(t) = \sum_{k=0}^K 64 a_{ik} t^3 (1-t)^3 \tilde{P}_k^{(6,6)}(t) \quad (18)$$

Then the terms of $\Delta\theta_i(t)$ form a system of functions which are orthogonal in the period of motion and satisfy the boundary conditions that the positions, velocities, and accelerations at the start and the goal are zero.

By the above reasoning, the minimum commanded torque change trajectory $\theta_i(t)$ is

$$\begin{aligned} \theta_i(t) &= \theta_i^s + (\theta_i^s - \theta_i^f)(-10t^3 + 15t^4 - 6t^5) \\ &\quad + 64 t^3 (1-t)^3 \sum_{k=0}^K a_{ik} \tilde{P}_k^{(6,6)}(t) \end{aligned} \quad (19)$$

Equation (19), which is the sum of the minimum angle jerk trajectory and the difference trajectory, always strictly satisfies boundary conditions (8). Letting the coefficient of the highest-order term be 1, the Jacobi polynomials $P_{k+1}^{(6,6)}(x)$ up to the $(k+1)$ -th are obtained as follows by the third-order recurrence formula [14]

$$\begin{aligned} P_0^{(6,6)}(x) &= 1 \\ P_1^{(6,6)}(x) &= x \\ P_2^{(6,6)}(x) &= x^2 - \frac{1}{15} \\ &\vdots \\ P_{k+1}^{(6,6)}(x) &= (x - \alpha_k)P_k^{(6,6)}(x) - \beta_k P_{k-1}^{(6,6)}(x) \end{aligned}$$

Here, we set $P_{-1}^{(6,6)}(x) = 0$, and

$$\begin{aligned} \alpha_k &= \frac{(xP_k^{(6,6)}(x), P_k^{(6,6)}(x))_w}{(P_k^{(6,6)}(x), P_k^{(6,6)}(x))_w} \quad (k = 0, 1, 2, \dots) \\ \beta_k &= \frac{(P_k^{(6,6)}(x), P_k^{(6,6)}(x))_w}{(P_{k-1}^{(6,6)}(x), P_{k-1}^{(6,6)}(x))_w} \quad (k = 1, 2, \dots) \end{aligned}$$

2.4. Estimation procedure for parameter a_{ik}

In order to estimate a_{ik} satisfying the Euler–Poisson equation, a method is proposed in which the coefficient a_{ik} is estimated by iterative calculation with the following two provisions:

- (1) The right-hand side of Eq. (5) is represented as a linear sum of a_{ik} .
- (2) The time during motion is discretized.

2.4.1. Linear sum of parameters a_{ik}

Substituting Eq. (19) into Eq. (5), the result is rearranged as in Eq. (20) which is linear with respect to a_{ik} :

$$\begin{aligned}
 E_1(t, \theta_1, \theta_2, \theta_1^{(1)}, \theta_2^{(1)}, \dots, \theta_1^{(3)}, \theta_2^{(3)}) \\
 &= \sum_{i=1}^2 \sum_{k=0}^K {}_1h_{ik}(t, \theta_1, \theta_2, \theta_1^{(1)}, \theta_2^{(1)}, \theta_1^{(2)}, \theta_2^{(2)}) a_{ik} \\
 &\quad + J_1(t, \theta_1, \theta_2, \theta_1^{(1)}, \theta_2^{(1)}, \dots, \theta_1^{(3)}, \theta_2^{(3)}) \\
 E_2(t, \theta_1, \theta_2, \theta_1^{(1)}, \theta_2^{(1)}, \dots, \theta_1^{(3)}, \theta_2^{(3)}) \\
 &= \sum_{i=1}^2 \sum_{k=0}^K {}_2h_{ik}(t, \theta_1, \theta_2, \theta_1^{(1)}, \theta_2^{(1)}, \theta_1^{(2)}, \theta_2^{(2)}) a_{ik} \\
 &\quad + J_2(t, \theta_1, \theta_2, \theta_1^{(1)}, \theta_2^{(1)}, \dots, \theta_1^{(3)}, \theta_2^{(3)}) \quad (20)
 \end{aligned}$$

Equation (20) is derived from Eqs. (5) and (19) by rearrangement according to the following criteria (A) and (B). Equation (19) is substituted only into $\theta_i^{(n)} (n=2, \dots, 6)$ satisfying criteria (A) and (B), and a_{ik} is represented as in Eq. (20).

(A) Substitution into $\theta_i^{(n)}$ such that $[1, A_1, A_2] \cdot \theta_i^{(n)} \cdot \theta_i^{(n)}$ represents the product of the terms in brackets and $\theta_i^{(n)}$. For A_1 and A_2 , see Table 1.

(B) Substitution into $\theta_i^{(4)}$ and $\theta_i^{(5)}$ of the term such that $[1, A_2, A_3] \cdot [\theta_i^{(4)} \cdot \theta_j^{(1)}, \theta_i^{(4)} \cdot (\theta_j^{(1)})^2, \theta_i^{(4)} \cdot \theta_1^{(1)} \cdot \theta_2^{(1)}, \theta_i^{(4)} \cdot \theta_j^{(2)}, \theta_i^{(5)} \cdot \theta_j^{(1)}] (i, j=1, 2)$. $[\cdot] \cdot [\cdot]$ represents the product of the terms in brackets. For A_2 and A_3 , see Table 1.

J_1 and J_2 are composed of terms into which Eq. (19) is not substituted by the above criteria and $(\theta_i^{AJ})^{(n)} (n=2, \dots, 6)$. More precisely, Table 1 shows the terms of which ${}_1h_{ik}$, ${}_2h_{ik}$, J_1 , and J_2 are composed.

2.4.2. Discretization of motion time

The normalized motion period is M -discretized with equal intervals with respect to time t as $[t_0, t_1, t_2, \dots, t_m, \dots, t_M] (t_0=0, t_M=1)$. If there exist parameters a_{ik} which represent the optimal trajectory of a motion, trajectory Eq. (20) satisfies Eq. (4). Then, the first equation of Eq. (20) satisfies

Table 1. Terms in ${}_1h_{ik}$, ${}_2h_{ik}$, J_1 , and J_2 . *: for the sagittal plane

${}_1h_{ik}$	Sum of terms A_1	*
${}_2h_{ik}$	Sum of terms $A_2, B_1, [A_2, A_3] \cdot B_1$	
J_1	Sum of terms $B_2, [A_1, A_4] \cdot B_2$	*
J_2	Sum of terms $B_3, [A_2, A_3] \cdot B_3$	
A_1	$\cos(\theta_1), \cos(\theta_1 + \theta_2), \cos^2(\theta_1), \cos^2(\theta_1 + \theta_2),$ $\cos(\theta_1) \cos(\theta_2), \cos(\theta_1) \cos(\theta_1 + \theta_2),$ $\cos(\theta_2) \cos(\theta_1 + \theta_2)$	
A_2	$\cos(\theta_2), \cos^2(\theta_2)$	
A_3	$\sin(\theta_2), \sin^2(\theta_2), \sin(\theta_2) \cos(\theta_2)$	
A_4	$\sin(\theta_1), \sin(\theta_1 + \theta_2), \sin(\theta_1) \cos(\theta_1),$ $\sin(\theta_1) \cos(\theta_1 + \theta_2), \cos(\theta_1) \sin(\theta_1 + \theta_2),$ $\sin(\theta_1) \sin(\theta_2), \sin(\theta_1) \cos(\theta_2), \cos(\theta_1) \sin(\theta_2),$ $\sin(\theta_2) \sin(\theta_1 + \theta_2), \sin(\theta_2) \cos(\theta_1 + \theta_2),$ $\cos(\theta_2) \sin(\theta_1 + \theta_2), \sin(\theta_1 + \theta_2) \cos(\theta_1 + \theta_2)$	
B_1	$\theta_1^{(1)}, \theta_2^{(1)}, (\theta_1^{(1)})^2, (\theta_2^{(1)})^2, \theta_1^{(1)} \theta_2^{(1)}$	
B_2	$(\theta_1^{(1)})^2, (\theta_2^{(1)})^2, \theta_1^{(1)} \theta_2^{(1)}, (\theta_1^{(1)})^3, (\theta_2^{(1)})^3,$ $(\theta_1^{(1)})^2 \theta_2^{(1)}, \theta_1^{(1)} (\theta_2^{(1)})^2, (\theta_1^{(1)})^4, (\theta_2^{(1)})^4, (\theta_1^{(1)})^3 \theta_2^{(1)},$ $\theta_1^{(1)} (\theta_2^{(1)})^3, (\theta_1^{(1)})^2 (\theta_2^{(1)})^2, (\theta_2^{(1)})^2, (\theta_2^{(2)})^2, \theta_2^{(1)} \theta_2^{(2)},$ $(\theta_1^{(1)})^2 \theta_2^{(2)}, \theta_1^{(2)} (\theta_2^{(1)})^2, \theta_1^{(1)} \theta_2^{(2)}, \theta_2^{(1)} \theta_2^{(2)}, \theta_1^{(1)} \theta_2^{(2)},$ $\theta_2^{(1)} \theta_2^{(2)}, \theta_1^{(1)} \theta_1^{(3)}, \theta_1^{(1)} \theta_2^{(3)}, \theta_2^{(1)} \theta_1^{(3)}, \theta_2^{(1)} \theta_2^{(3)},$ $(\theta_1^{(1)})^2 \theta_2^{(2)}, \theta_1^{(2)} (\theta_2^{(2)})^2, \theta_1^{(1)} \theta_2^{(1)} \theta_2^{(2)}, \theta_1^{(1)} \theta_2^{(1)} \theta_2^{(2)},$ $(\theta_i^{AJ})^{(2)}, (\theta_i^{AJ})^{(3)}, (\theta_i^{AJ})^{(4)} (i=1, 2)$	
B_3	$(\theta_2^{(1)})^5, \theta_1^{(1)} (\theta_2^{(1)})^4, (\theta_1^{(1)})^2 (\theta_2^{(1)})^3, \theta_1^{(2)} (\theta_2^{(1)})^3,$ $(\theta_2^{(1)})^3 \theta_2^{(2)}, (\theta_1^{(1)})^2 \theta_2^{(1)}, \theta_1^{(1)} (\theta_2^{(2)})^2, \theta_2^{(1)} (\theta_2^{(2)})^2,$ $(\theta_1^{(1)})^2 \theta_2^{(3)}, (\theta_2^{(1)})^2 \theta_2^{(3)}, (\theta_1^{(1)})^2 \theta_2^{(3)}, (\theta_2^{(1)})^2 \theta_2^{(3)},$ $\theta_1^{(2)} \theta_1^{(3)}, \theta_2^{(2)} \theta_1^{(3)}, \theta_1^{(2)} \theta_2^{(3)}, \theta_2^{(2)} \theta_2^{(3)}, \theta_1^{(1)} \theta_1^{(2)} \theta_2^{(2)},$ $\theta_2^{(1)} \theta_2^{(2)} \theta_2^{(2)}, \theta_1^{(1)} \theta_2^{(1)} \theta_1^{(3)}, \theta_1^{(1)} \theta_2^{(1)} \theta_2^{(3)},$ $\theta_1^{(1)} (\theta_2^{(1)})^2 \theta_2^{(2)}, (\theta_1^{(1)})^2 \theta_2^{(1)} \theta_2^{(2)}, \theta_1^{(1)} (\theta_2^{(1)})^2 \theta_2^{(2)},$ $(\theta_2^{(1)})^6, \theta_1^{(1)} (\theta_2^{(1)})^5, (\theta_1^{(1)})^4 (\theta_2^{(1)})^2, (\theta_1^{(1)})^2 (\theta_2^{(1)})^4,$ $(\theta_1^{(1)})^3 (\theta_2^{(1)})^3, \theta_1^{(2)} (\theta_2^{(1)})^4, (\theta_1^{(1)})^4 \theta_2^{(2)}, (\theta_2^{(1)})^4 \theta_2^{(2)},$ $(\theta_1^{(1)})^2 (\theta_2^{(2)})^2, (\theta_2^{(1)})^2 (\theta_2^{(2)})^2, (\theta_1^{(1)})^2 (\theta_2^{(2)})^2,$ $(\theta_2^{(1)})^2 (\theta_2^{(2)})^2, (\theta_2^{(1)})^3, (\theta_2^{(2)})^3, (\theta_1^{(2)})^2 \theta_2^{(2)},$ $\theta_1^{(2)} (\theta_2^{(2)})^2, (\theta_1^{(1)})^3 \theta_1^{(3)}, (\theta_2^{(1)})^3 \theta_1^{(3)}, (\theta_1^{(1)})^3 \theta_2^{(3)},$ $(\theta_2^{(1)})^3 \theta_2^{(3)}, (\theta_1^{(3)})^2, (\theta_2^{(3)})^2, \theta_1^{(3)} \theta_2^{(3)},$ $(\theta_1^{(1)})^3 \theta_1^{(2)} \theta_2^{(1)}, \theta_1^{(1)} \theta_1^{(2)} (\theta_2^{(1)})^3, (\theta_1^{(1)})^3 \theta_1^{(1)} \theta_2^{(2)},$ $\theta_1^{(1)} (\theta_2^{(1)})^3 \theta_2^{(2)}, (\theta_1^{(1)})^2 \theta_2^{(2)} (\theta_2^{(1)})^2,$ $(\theta_1^{(1)})^2 (\theta_2^{(1)})^2 \theta_2^{(2)}, (\theta_1^{(1)})^2 \theta_2^{(1)} \theta_2^{(2)},$ $\theta_1^{(1)} \theta_2^{(1)} (\theta_2^{(1)})^2, \theta_1^{(1)} \theta_2^{(1)} (\theta_2^{(2)})^2,$ $(\theta_1^{(1)})^2 \theta_2^{(1)} \theta_2^{(3)}, \theta_1^{(1)} (\theta_2^{(1)})^2 \theta_2^{(3)}, (\theta_1^{(1)})^2 \theta_2^{(1)} \theta_2^{(3)},$ $\theta_1^{(1)} (\theta_2^{(1)})^2 \theta_2^{(3)}, \theta_1^{(1)} \theta_1^{(2)} \theta_2^{(3)}, \theta_2^{(1)} \theta_2^{(3)} \theta_2^{(1)},$ $\theta_1^{(1)} \theta_1^{(3)} \theta_2^{(2)}, \theta_1^{(1)} \theta_1^{(2)} \theta_2^{(3)}, \theta_1^{(3)} \theta_2^{(1)} \theta_2^{(2)}, \theta_1^{(1)} \theta_2^{(2)} \theta_2^{(3)},$ $\theta_1^{(2)} \theta_2^{(1)} \theta_2^{(3)}, \theta_2^{(1)} \theta_2^{(2)} \theta_2^{(3)}, \theta_1^{(1)} \theta_2^{(1)} \theta_1^{(2)} \theta_2^{(2)},$ $(\theta_i^{AJ})^{(4)}, (\theta_i^{AJ})^{(5)}, (\theta_i^{AJ})^{(6)}, (\theta_i^{AJ})^{(4)} \theta_1^{(1)},$ $(\theta_i^{AJ})^{(4)} \theta_2^{(1)}, (\theta_i^{AJ})^{(4)} (\theta_1^{(1)})^2, (\theta_i^{AJ})^{(4)} (\theta_2^{(1)})^2,$ $(\theta_i^{AJ})^{(4)} \theta_1^{(1)} \theta_2^{(1)}, (\theta_i^{AJ})^{(5)} \theta_1^{(1)}, (\theta_i^{AJ})^{(5)} \theta_2^{(1)}, (i=1, 2)$	

$$\sum_{i=1}^2 \sum_{k=0}^K {}_1h_{ik}(t_m, \theta_{1m}, \theta_{2m}, \theta_{1m}^{(1)}, \theta_{2m}^{(1)}, \theta_{1m}^{(2)}, \theta_{2m}^{(2)}) a_{ik} + J_1(t_m, \theta_{1m}, \theta_{2m}, \theta_{1m}^{(1)}, \theta_{2m}^{(1)}, \dots, \theta_{1m}^{(3)}, \theta_{2m}^{(3)}) = 0 \quad (0 \leq m \leq M) \quad (21)$$

Using ${}_1h_{ikm} = {}_1h_{ik}(t_m, \dots)$ and $J_{1m} = J_1(t_m, \dots)$, the above relation is written as

$$\sum_{i=1}^2 \sum_{k=0}^K {}_1h_{ikm} a_{ik} + J_{1m} = 0 \quad (22)$$

Similarly, using ${}_2h_{ikm} = {}_2h_{ik}(t_m, \dots)$ and $J_{2m} = J_2(t_m, \dots)$, the second equation of Eq. (20) is written as

$$\sum_{i=1}^2 \sum_{k=0}^K {}_2h_{ikm} a_{ik} + J_{2m} = 0 \quad (23)$$

At any discretized time, Eqs. (22) and (23) must hold. Thus, a system of $2(M+1)$ linear equations is derived, which is represented as follows in matrix form:

$$\begin{bmatrix} {}_1h_{100} & \dots & {}_1h_{2K0} \\ \vdots & \ddots & \vdots \\ {}_1h_{10m} & \dots & {}_1h_{2Km} \\ \vdots & \ddots & \vdots \\ {}_1h_{10M} & \dots & {}_1h_{2KM} \\ {}_2h_{100} & \dots & {}_2h_{2K0} \\ \vdots & \ddots & \vdots \\ {}_2h_{10m} & \dots & {}_2h_{2Km} \\ \vdots & \ddots & \vdots \\ {}_2h_{10M} & \dots & {}_2h_{2KM} \end{bmatrix} \begin{bmatrix} a_{10} \\ a_{11} \\ \vdots \\ a_{1K} \\ a_{20} \\ \vdots \\ a_{2K} \end{bmatrix} + \begin{bmatrix} J_{10} \\ \vdots \\ J_{1m} \\ \vdots \\ J_{1M} \\ J_{20} \\ \vdots \\ J_{2m} \\ \vdots \\ J_{2M} \end{bmatrix} = \mathbf{0} \quad (24)$$

$$\mathbf{H}\mathbf{a} + \mathbf{J} = \mathbf{0}$$

Thus,

$$\mathbf{a} = -\mathbf{H}^\# \mathbf{J} \quad (24)$$

where $\mathbf{H}^\#$ is the pseudoinverse matrix of \mathbf{H} .

Equation (5) is rearranged as a linear sum of a_{ik} . Using Eq. (24), which is derived by discretizing the movement time, the parameters a_{ik} of the optimal trajectory are estimated. a_{ik} is estimated by the following iterative calculation.

(1) The initial value of the parameter a_{ik} is set as 0, and the joint angle trajectory θ_i is calculated from Eq. (19).

(2) For each time t_m ($m=0, 1, \dots, M$), ${}_1h_{ikm}$, ${}_2h_{ikm}$, J_{1m} , and J_{2m} are calculated.

(3) a_{ik} is determined from Eq. (24).

(4) The new joint angle trajectory θ_i for the a_{ik} determined in step (3) is calculated by Eq. (19).

Steps (2) to (4) are iterated until a_{ik} converges. That is, letting the index of the iterations be d ($d=0, 1, 2, \dots$), it follows from Eq. (21) that

$$\mathbf{a}^{d+1} = -\mathbf{H}(\mathbf{a}^d)^\# \mathbf{J}(\mathbf{a}^d) \quad (25)$$

3. Numerical Experiments

Numerical experiments were performed for the following two cases.

(1) For the same start, goal, and duration of motion as in the data measured by Nakano and colleagues [5], the minimum commanded torque change trajectory is generated.

(2) For the specified start, goal, and duration of motion, the minimum commanded torque change trajectory is experimentally generated by varying the viscosity.

First, in order to assess the predicted trajectory, the error of the Euler–Poisson equation is defined as the maximum absolute value of the error:

$$\begin{aligned} & \max_{0 \leq t_m \leq 1} \sum_{i=1}^2 |E_i^*(t_m) - E_i(t_m)| \\ &= \max_{0 \leq t_m \leq 1} \sum_{i=1}^2 |0 - E_i(t_m)| \\ &= |\mathbf{E}|_{\max} \end{aligned} \quad (26)$$

Here, $E_i^*(t_m)$ is the value of $E_i(t_m)$ on the optimal trajectory. As is obvious from Eq. (4), we have $E_i^*(t) = 0$ ($0 \leq t \leq 1$). Whether or not the trajectory satisfies the Euler–Poisson equation is decided in terms of this measure.

3.1. Numerical experiment 1

In this numerical experiment, the start and goal of the motion trajectory and the dynamical parameters of three subjects as measured in the study of Nakano and colleagues [5] were used. The motion planes were (a) the horizontal plane and (b) the sagittal plane as shown in Fig. 1. The number of trajectories was 200 for each plane. Therefore, 1200 minimum commanded torque change trajectories were generated.

The dynamical parameters are shown in Table 2. The value of the viscosity B_{ij} is taken from Gomi and Osu [15]. The diagonal elements B_{11} and B_{22} are 0.6 to 1.2 Nm/rad,

Table 2. Dynamics parameters

Parameter	Subject			
	Link i	1	2	3
L_i [m]	1	0.285	0.265	0.300
	2	0.335	0.330	0.345
M_i [kg]	1	1.41	1.30	1.50
	2	1.08	1.07	1.11
S_i [m]	1	0.107	0.099	0.113
	2	0.164	0.161	0.168
I_i [kg · m ²]	1	0.0248	0.0195	0.0294
	2	0.0433	0.0415	0.0469

and the nondiagonal elements $B_{12}(= B_{21})$ are 0.06 to 0.3 Nm/rad.

First, the relation between the number of parameters K and the error $|\mathcal{E}|_{\max}$ is examined. Equation (11) or (18) is used as the difference trajectory. K is set as 10, 12, 14, . . . , 70. The initial values of a'_{ik} and a_{ik} are set as 0. Then the trajectory is generated by iterative calculation using Eq. (25).

Figure 2 shows the error $|\mathcal{E}|_{\max}$ as a function of the number of parameters K . The horizontal axis is the number of parameters K and the vertical axis is $|\mathcal{E}|_{\max}$ calculated by Eq. (26). A to D in the figure correspond, respectively, to the four trajectories shown in Fig. 4. In the two difference trajectories given by Eqs. (11) and (18), $|\mathcal{E}|_{\max}$ tends to decrease with increasing K . Compared to the case in which Eq. (11) is used, $|\mathcal{E}|_{\max}$ is more stable when Eq. (18) is used. When Eq. (18) is used, $|\mathcal{E}|_{\max}$ almost converges for $K = 54$,

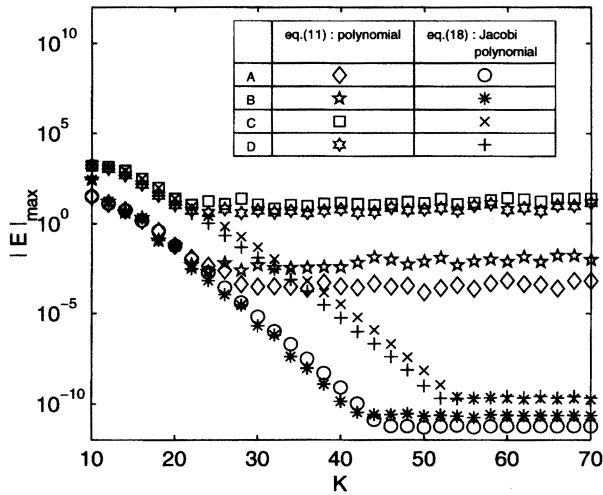


Fig. 2. Relationship between the number of parameters K and $|\mathcal{E}|_{\max}$. A to D: trajectories in Fig. 4.

and the derived trajectory is seen to satisfy the Euler–Poisson equation with very high accuracy. It seems that the optimal number of parameters K differs depending on the trajectory. Consequently, in the following, the number of parameters K that minimizes the error $|\mathcal{E}|_{\max}$ is sought.

Using 1200 starts, goals, and durations of motion measured by Nakano and colleagues [15], the minimum commanded torque change trajectories were generated by the proposed method, the Newton-like method, and the method of steepest descent.

Figure 3 shows the convergence of the error $|\mathcal{E}|_{\max}$ in 100 iterative calculations. The horizontal axis is the number of updates of the parameter a_{ik} , and the vertical axis is $|\mathcal{E}|_{\max}$ calculated by Eq. (26). A to D of the figure correspond, respectively, to the four trajectories shown in Fig. 4. The slopes of descent of $|\mathcal{E}|_{\max}$ seem almost the same in all trajectories derived by Eqs. (11) and (18), but the error of Eq. (11) converges to a relatively large value, while that of Eq. (18) converges to a very small value, less than 10^{-9} . In other words, the trajectory obtained by the latter procedure satisfies the Euler–Poisson equation with high accuracy at any time in the duration of motion. When Eq. (18) is used, the error converges to a very small value after as few as 20 iterations.

Thus, we see that a system of orthogonal polynomials such as the Jacobi polynomials is effective in the method proposed in this paper. For the trajectories which can be derived by the Newton-like method, as well as these which cannot, the proposed method can generate a trajectory satisfying the Euler–Poisson equation with higher numerical accuracy in the same number of iterations.

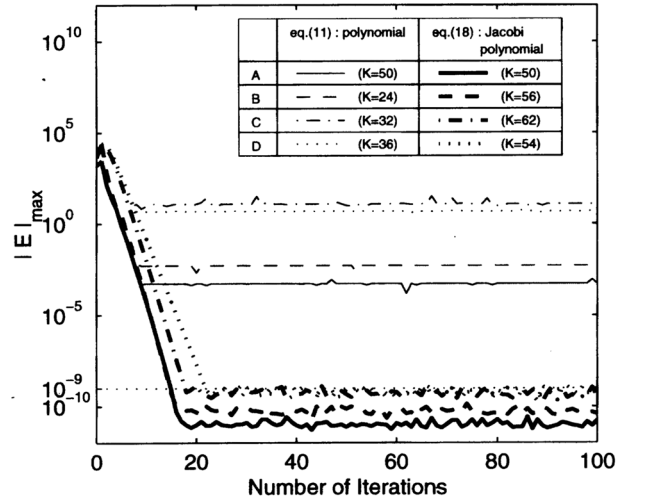


Fig. 3. Convergence of $|\mathcal{E}|_{\max}$. A to D: trajectories in Fig. 4.

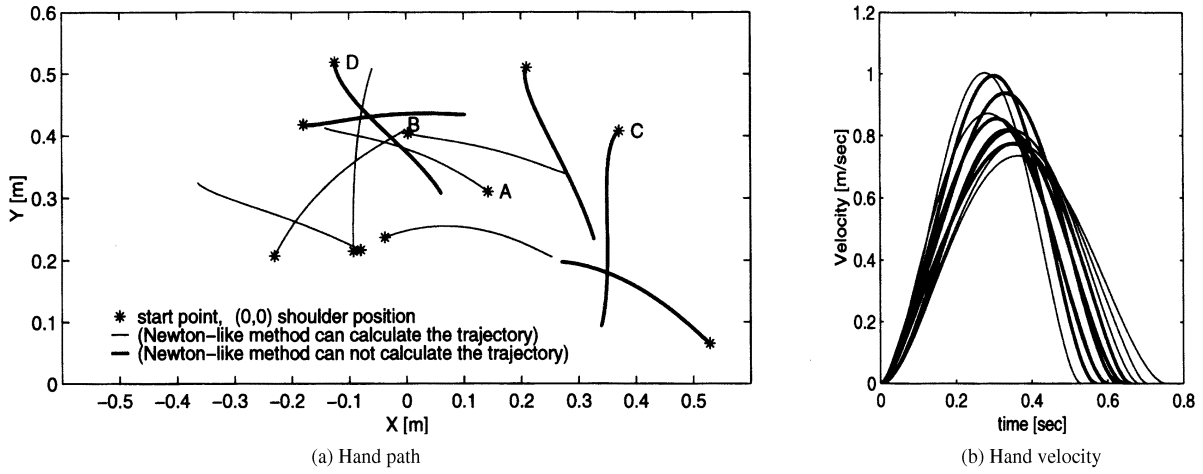


Fig. 4. Minimum commanded torque change trajectories calculated using the proposed method in the horizontal plane.

Figure 4 shows the minimum commanded torque change trajectory on the horizontal plane obtained by the proposed method. In (a), the Y axis is the front direction of the body with the origin at the shoulder. As is shown by the thick line, a trajectory is obtained that satisfies the Euler–Poisson equation with high accuracy between the start and the goal, for which no optimal solution has been obtained. It is also seen that the feature of the human arm motion that the trajectory is almost a straight line but is slightly curved, and also the feature that the velocity waveform with respect to time is of a single-peaked bell shape, are well reproduced.

As in Fig. 3, trajectories with very small $|E|_{\max}$ are also obtained in the sagittal plane. Twelve hundred trajectories for all motions in the horizontal and sagittal planes are derived with small errors, as shown in Fig. 3.

Table 3 shows examples of the values of the evaluation function (square integral of commanded torque change) for the trajectories derived by various methods, for

Table 3. Values of the performance index (the time integral of square of the commanded torque change rate). A dash indicates that the method cannot calculate the optimal trajectory

Horizontal plane	1	2
The proposed method	33.4432	92.1030
Newton-like method	33.4432	—
Steepest descent method	33.4619	92.1660
Sagittal plane	1	2
The proposed method	93.7844	40.3807
Newton-like method	93.7845	—
Steepest descent method	93.8458	40.3932

the horizontal and sagittal planes. For the trajectories generated from the difference trajectory by Eqs. (11) and (18), the values of the evaluation function are almost the same. We see that in either case the value of the evaluation function is not greater in the method proposed in this paper. It is also verified that a convergent solution is obtained by the proposed method for the case in which the trajectory cannot be obtained by the Newton-like method.

In order to see how the Euler–Poisson equation is satisfied by the proposed method based on the difference trajectory of Eq. (11) or (18) and the Newton-like method, E_1 and E_2 [Eq. (5)] are calculated for each time. Since the solution by the Newton-like method is a numerical solution, the time derivatives up to sixth derivative of the joint angle are obtained by five-point numerical differentiation.

Figure 5 shows the absolute values of E_1 and E_2 at each time, obtained by the proposed method and the Newton-like method. The horizontal axis is the normalized time and the vertical axis represents the absolute values of E_1 and E_2 [Eq. (5)]. Compared to the case in which Eq. (18) is used, we see that the error is larger over the whole motion period when Eq. (11) is used. It is evident that the result given by Eq. (11) satisfies the Euler–Poisson equation with much higher accuracy than that given by the Newton-like method over the whole motion period.

3.2. Numerical experiment 2

In the previous section, the trajectory was generated on the basis of the measured data. In this section we investigate the stability of the result to changes of the dynamical parameters in the proposed method; the examination is focused on the change of the viscosity, which is a

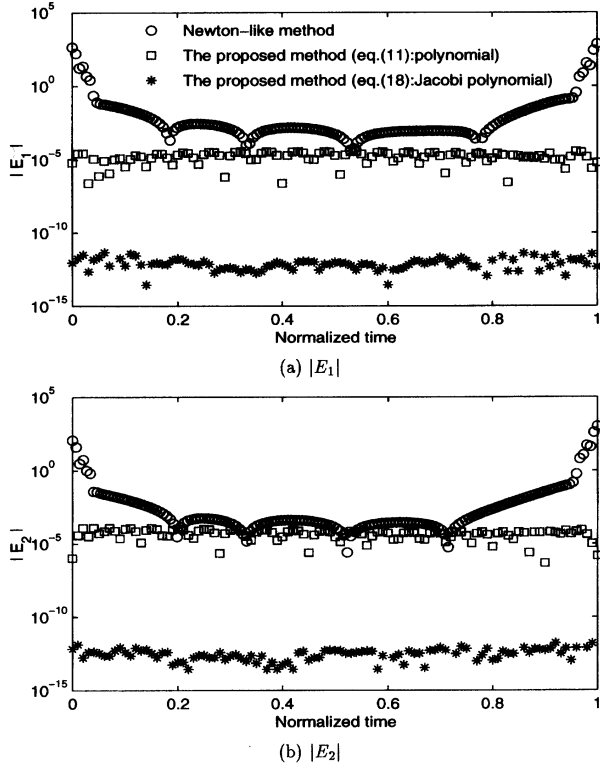


Fig. 5. Absolute values of E_1 and E_2 (trajectory A in Fig. 4).

- : Newton-like method;
- : the proposed method with Eq. (11);
- *: the proposed method with Eq. (18).

major factor responsible for the inability of the Newton-like method to derive a convergent solution. The start, the goal, and the duration of motion are set as follows, and the minimum commanded torque change trajectory is generated while varying the viscosity.

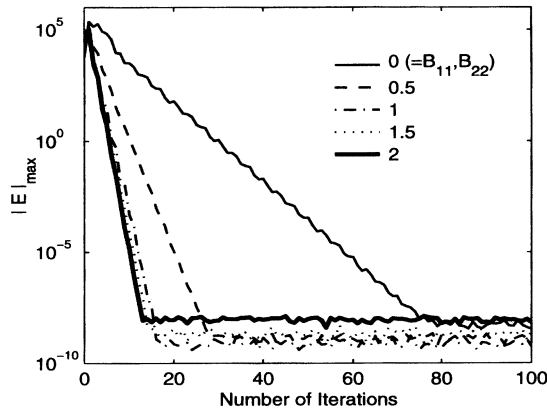


Fig. 6. Convergence of $|E|_{\max}$ when the values of viscosity B_{11} , B_{22} change.

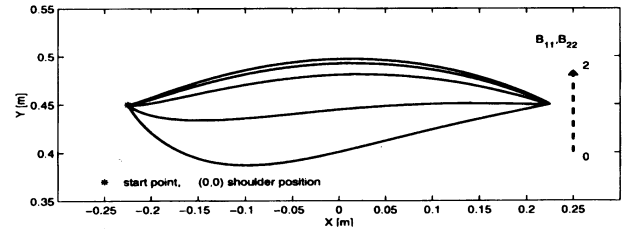


Fig. 7. Minimum commanded torque change trajectories when the values of viscosity B_{11} , B_{22} are 0, 0.5, 1.0, 1.5, and 2 Nm/rad.

*: start point; origin: shoulder position.

As dynamical parameters, the values of Subject 1 of Table 2 in numerical experiment 1 are used. As the value of the viscosity B_{ij} , the diagonal elements are set as $B_{11} = B_{22}$ with the value varied as 0, 0.1, 0.2, . . . , 2 Nm/rad. The nondiagonal element $B_{12}(=B_{21})$ is set as 0. The motion duration is set as $t_f = 0.5$ s. It is assumed that the hand is moved from $(x = -0.225$ m, $y = 0.450$ m) to $(x = 0.225$ m, $y = 0.450$ m). The number of parameters K and the initial value of a_{ik} are set the same as in numerical experiment 1 in performing the iterative calculation.

Figure 6 shows the convergence of the error $|E|_{\max}$ in 100 iterative calculations. The horizontal axis is the number of updates of parameter a_{ik} and the vertical axis is $|E|_{\max}$ calculated by Eq. (26). As in numerical experiment 1, the convergence value of $|E|_{\max}$ is very small, being of the order of 10^{-8} , indicating that the derived trajectory satisfies the Euler–Poisson equation with high accuracy at any time in the motion duration.

Figure 7 shows the minimum commanded torque change trajectories for viscosities B_{11} and B_{22} of 0, 0.5, 1, 1.5, 2 Nm/rad. The coordinate is the same as in Fig. 4(a). The value of B_{11} and B_{22} is larger in the trajectories following the dashed arrow. We see that the trajectory is curved farther away from the body when B_{11} and B_{22} are large, and is nearer when they are small. This numerical experiment verifies that the proposed method is an algorithm that derives the solution stably even if the viscosity is varied.

4. Conclusions

A method is proposed which can generate a trajectory that satisfies the Euler–Poisson equation with high accuracy. It is shown by numerical experiments that the proposed method has the following advantages. The trajectory obtained by the proposed method is the same as the trajectory obtained by the Newton-like method, which is mathematically guaranteed for accuracy. Even when a convergent

trajectory is not obtained by the Newton-like method, a trajectory is obtained that satisfies the Euler–Poisson equation with high accuracy. The derived solution strictly satisfies the boundary conditions.

The value of the viscosity, which is one of the factors preventing the convergence of the solution in the Newton-like method, is varied over a wide range, and it is verified that the proposed method can derive the solution stably. Compared to the methods proposed previously, it is seen that the proposed method can determine a convergent solution in a very short time. In this paper, the value of K is varied and the value that produces the smallest error is determined. As is shown in Fig. 2, however, it is sufficient to set approximately $K = 60$. Consequently, it is not necessary to search for the optimal value. It is possible to derive a solution that satisfies the Euler–Poisson equation with high accuracy.

The method proposed in this paper is a general procedure for deriving a solution for a nonlinear optimization problem, and can be applied to various problems. Depending on the composition of h and J in Table 1, however, it may happen that the procedure does not converge. It is left as an important issue to clarify theoretically the conditions for convergence. It seems that the proposed method can be applied to motion with a via-point. It is of interest to attempt optimization considering the via-point time in order to extend the proposed method to a procedure for generating more general trajectories.

Acknowledgments. The authors thank members of the ERATO Kawato Learning Dynamics Project, ATR Human Information Processing Research Laboratories, for providing them the opportunity to perform this research and for useful advice. This study was supported in part by a grant from the Science and Technology Agency under the project “Study of Communication of Primates, Including Humans.”

REFERENCES

1. Abend W, Bizzi E, Morasso P. Human arm trajectory formation. *Brain* 1982;105:331–348.
2. Flash T, Hogan N. The coordination of arm movements: An experimentally confirmed mathematical model. *J Neurosci* 1985;5:1688–1703.
3. Rosenbaum DA, Loukopoulos LD, Meulenbroek RG, Vaughan J, Engelbrecht SE. Planning reaches by evaluating stored posture. *Psychol Rev* 1995;102:28–67.
4. Uno Y, Kawato M, Suzuki R. Formation and control of optimal trajectory in human multijoint arm movement—minimum torque-change model. *Biol Cybern* 1989;61:89–101.
5. Nakano E, Imamizu H, Osu R, Uno Y, Gomi H, Yoshioka T, Kawato M. Quantitative examinations of internal representations for arm trajectory planning: Minimum commanded torque change model. *J Neurophysiol* 1999;81:2140–2155.
6. Bizzi E, Accornero N, Chapple W, Hogan N. Posture control and trajectory formation during arm movement. *J Neurosci* 1984;4:2738–2744.
7. Sakuraba H, Osu E, Nakano E, Wada Y, Kawato M. Characterization of fingertip trajectory by control of incomplete inverse dynamics model. *Trans IEICE* 2000;J83-D-II:784–794.
8. Mitsui T. Boundary value problems of differential equations and Newton’s method. *Math Sci* 1981;19:41–46.
9. Uno Y, Kawato M, Suzuki R. Iterative motion control for optimal trajectory of robot manipulator. *Proc Soc Autom Control* 1988;24:837–843.
10. Uno Y, Kawato M. A hybrid method for calculating optimal trajectories. 8th Natl Conv, Soc Neural Networks, p 154–155, 1997.
11. Sakurai A. Introduction to spline functions. Tokyo Denki University; 1989.
12. Kaneko Y, Nakano E, Osu R, Wada Y, Kawato M. Generation of minimum elastic torque change trajectory using the Euler–Poisson equation. *Proc Conv IEICE, Hokuriku Chapter*, p 67–68, 1998.
13. Mori M, Sugihara M, Murota K. Linear computation. Iwanami Shoten; 1994.
14. Sugibara M, Murota K. Mathematics of numerical calculation, 2nd ed. Iwanami Shoten; 1998.
15. Gomi H, Osu R. Task dependent viscoelasticity of human multijoint-arm and its spatial characteristics for interaction with environments. *J Neurosci* 1998;18:8965–8978.

AUTHORS (from left to right)



Yuichi Kaneko (student member) received his B.S. degree from the Department of Electronic Instrumentation, Nagaoka University of Technology, in 1998 and is now an M.E. candidate. He is engaged in research on motion control and nonlinear systems.

Eri Nakano completed her M.E. program at the Graduate School of Arts, Kobe University, in 1996 and entered the doctoral program at the Graduate School of Natural Science. She was dispatched as a research student to ATR Human Information Processing Research Laboratories. In 1999, she was a visiting researcher at the International Advanced Telecommunications Research Institute. She has been engaged in research on biological motion functions. She is a member of the Japan Psychological Society, Japan Neural Science Society, and North American Society for Neural Science.

Rieko Osu obtained her research guidance qualification in the doctoral program at the Graduate School of Arts, Kyoto University, in 1996 and joined ATR Human Information Processing Research Laboratories. She is now a researcher with the ERATO Kawato Dynamic Brain Project, and is engaged in research on biological motion functions. She is a member of the Japan Psychological Society, Japan Neural Science Society, and North American Society for Neural Science.

Yasuhiro Wada (member) received his B.S. degree from the Department of Control Engineering, Tokyo Institute of Technology, in 1980, completed the M.E. program (system science) in 1982, and joined Kawasaki Steel Company. He moved to ATR Visual and Auditory Function Research Laboratory in 1989, and to ATR Human Information Processing Research Laboratories in 1992. He has been an associate professor at Nagaoka University of Technology since 1997, and is engaged in research on motion control and neural networks. He holds a D.Eng. degree, and is a member of the Neural Network Society and Society of Instrument and Control Engineers.

Mitsuo Kawato (member) completed the doctoral program at the Graduate School of Engineering Science, Osaka University, in 1981. After serving there as a research associate and lecturer, he moved to ATR Visual and Auditory Research Laboratory in 1988, serving as head of the 3rd Laboratory. In 1992 he joined ATR Human Information Processing Research Laboratory. He was a visiting professor at the Electronic Science Institute, Hokkaido University, from 1992 to 1995; at the University of Genoa, Italy, in 1993; and at Kanazawa Institute of Technology in 1994. Since 1996, he has held an adjunct appointment as organizer, ERATO Kawato Dynamic Brain Project, and is engaged in research on computational neural science of the brain. He has received the Yonezawa Prize, Osaka Science Award, Ministerial Award Science and Technology Agency, and Tsukahara Prize. He is the editor of the *Journal of Neural Networks*, and editorial executive and Prize Selection Committee member, Neural Network Society.